Available online at www.sciencedirect.com
ScienceDirect
Journal of Environmental Sciences 2010, 22(12) 1846–1853
JOURNAL OF ENVIRONMENTAL SCIENCES
ISSN 1001-0742
CN 11-2629/X
www.jesc.ac.cn

Removal of bromate ion using powdered activated carbon

Lian Wang[1,2], Jie Zhang[2], Jingze Liu[1,*], Hong He[2], Min Yang[2], Jianwei Yu[2], Zichuan Ma[3], Feng Jiang[4]

1. College of Life Science, Hebei Normal University, Shijiazhuang 050016, China. E-mail: lianwang@mail.ustc.edu.cn
2. Research Center for Eco-Environmental Sciences, Chinese Academy of Sciences, Beijing 100085, China
3. College of Chemistry & Material Science, Hebei Normal University, Shijiazhuang 050016, China
4. Beijing YADU Indoor Environmental Protection Science and Technology Co., Ltd., Beijing 102206, China

Received 08 January 2010; revised 16 April 2010; accepted 20 April 2010

Abstract

Bromate ion (BrO_3^-) removal from drinking water by powdered activated carbons (PAC_S) in bath mode was evaluated under various operational conditions. Six kinds of PACs, including wood-based carbon, fruit-based carbon, coal-based carbon, and these three carbons thermally deoxidized in a nitrogen atmosphere, were selected to investigate their capacity on BrO_3^- removal. With the highest zeta potential value and being richly mesoporous, coal-based carbon had a high and an excellent BrO_3^- adsorption efficiency. The removal content of BrO_3^- by per gram of coal-based carbon was 0.45 mg within 5 hr in 100 μg/L bromate solution. The surface characteristics of PACs and bromide formation revealed that both physical and chemical PACs properties simultaneously affected the adsorption-reduction process. Under acidic conditions, PAC_S possessed high zeta value and adequate basic groups and exhibited neutral or positive charges, promoting BrO_3^- adsorption-reduction on the carbon surface. Interestingly, the PAC_S thermally deoxidized in N_2 atmosphere optimized their properties, e.g. increasing their zeta values and decreasing the oxygen content which accelerated the BrO_3^- removal rate. The maximum adsorption capacity of fruit-based carbon was the highest among all tested carbons (99.6 mg/g), possibly due to its highest pore volume. Remarkably, the thermal regeneration of PACs in N_2 atmosphere could completely recover the adsorption capacity of PACs. The kinetic data obtained from carbons was analyzed using pseudo second-order and intraparticle diffusion models, with results showing that the intraparticle diffusion was the more applicable model to describe adsorption of BrO_3^- onto PACs.

Key words: bromate; powdered activated carbons; adsorption-reduction process; adsorption capacity
DOI: 10.1016/S1001-0742(09)60330-2

Introduction

The presence of bromate in drinking water has attracted much attention because it is an animal carcinogen (Marhaba and Bengraïne, 2003; Wolf et al., 1998). In the process of ozonation, bromate can be formed through complex reactions on molecular ozone and hydroxyl radical (von Gunten and Hoignè, 1994). Ozonation is a disinfection method that can destroy microorganisms, reduce the color, odor, and total organic carbon, etc. In the process of ozonation, bromide is oxidized to hypobromous acid and hypobromite, which are further oxidized to bromate by ozone and/or hydroxyl radicals. In general, the concentration of bromate in drinking water ranges from 0.4 to 100 μg/L (Butler et al., 2005; Krasner et al., 1993). A maximum allowed contaminant level of bromate is 10 μg/L by the European Union (1980), while the World Health Organization set a provisional guideline value of 25 μg/L (WHO, 1996).

Up to now, three approaches have been used to reduce the concentration of bromate in water. One approach is to remove the bromate precursors, such as bromide and natural organic matter before ozonation process (Johnson and Singer, 2004; Marhaba and Bengraïne, 2003). The second one is to control the bromate formation during ozonation through pH control by adding ammonia or hydrogen peroxide, and by modifying ozonation operation (Bouland et al., 2003; Kim et al., 2007). The third approach is using physical and chemical methods to remove bromate after ozonation. Most research works have been focused on the use of activated carbons (especially granular activated carbon) to remove bromate owing to the high removal efficiency of activated carbon (Bao et al., 1999; Huang et al., 2007; Huang and Cheng, 2008; Kirisits et al., 2000; Siddiqui et al., 1996). However, the granular activated carbon capacity is carbon-specific and depends on the source water (Bao et al., 1999; Kirisits et al., 2000).

The mechanisms of BrO_3^- removal by activated carbon have been proposed by some researchers (Bao et al., 1999; Kirisits et al., 2000; Siddiqui et al., 1996; Studebaker, 1957). It has been widely accepted that the removal of BrO_3^- by activated carbon is postulated to be adsorbed first, then reduced to hypobromite (BrO^-), and finally

* Corresponding author. E-mail: liujingze@mail.hebtu.edu.cn

reduced to bromide (Br^-) on activated carbon surface (Siddiqui et al., 1996). Previous report found that activated carbons with less surface oxygen tend to be basic and have an anion exchange capacity because of their positive charge (Chingombe et al., 2005). It means that some reduction methods such as N_2 reduction treatment could decrease the surface oxygen of activated carbons, such that increase the removal rate of BrO_3^- on activated carbons. Moreover, Siddiqui et al. (1996) concluded that the increase in the acidity of carbon could compromise the adsorption of BrO_3^- due to unfavorable electrostatic interactions between anions and acid groups. Huang et al. (2007) reported that the removal capacity of BrO_3^- increased with decreasing solution pH. Therefore, further work is needed to confirm the effects of the acidity and basicity of carbon surface on BrO_3^- removal with the pH variation. In addition, the works on the maximum removal capacity, reproduction capacity, and kinetics of powdered activated carbon, that are important factors for optimization selection to remove BrO_3^-, are still limited.

The purpose of this study was to elucidate how the physical and chemical characteristics of powdered activated carbon influence BrO_3^- removal in bath mode. Six kind of powdered activated carbons (PACs) (wood-based carbon, fruit-based carbon, coal-based carbon, and three carbons thermally deoxidized in N_2 atmosphere) were characterized using nitrogen adsorption, X-ray photoelectron spectroscopy (XPS), zeta potential measurement, and acid-base titrations. The adsorption capacities of the various PACs were compared and the adsorption kinetics of BrO_3^- on PACs were developed.

1 Experimental

1.1 Materials

Three types of commercial PACs, wood-based carbon (PAC_W) (Shanxi Xinhua Carbon Corporation, China), one fruit-based carbon (PAC_F) (Tangshan Huaneng Carbon Corporation, China), and one coal-based carbon (PAC_C) (Ningxia Taixi Carbon Corporation, China) were used in this study. Prior to experiments, the samples were washed using ultra-pure water and dried overnight at 110°C to remove excess water, then cooled and stored in a desiccator. In order to determine their surface characteristics, the above three carbons were thermally treated at 600°C in N_2 environment at a flow rate of 100 mL/min for 3 hr. Then the samples were cooled to room temperature in N_2 atmosphere and stored in a desiccator.

1.2 Characterization of activated carbons

The surface area and pore size distribution of PACs samples were determined through nitrogen adsorption/desorption isotherms at –196°C using Quantasorb-18 automatic equipment (Quanta Chrome Instrument Co., USA). All samples were initially outgassed at 300°C for 6 hr in vacuum. The specific surface areas were calculated from these isotherms by applying the Brunauer-Emmett-Teller (BET) method. The pore size distribution and mesopore volume (V_{meso}) were evaluated by applying the Dollimore-Heal method (Dollimore and Heal, 1964) to desorption isotherm, whereas the *t*-plot approach (Lippens and de Boer, 1965) was adopted to estimate micropore volume (V_{micro}).

Zeta potential of the PACs in ultra-pure water was measured with a Zetasizer 2000 (Malvern Co., UK). The concentration of PACs was 200 mg/L. The measurements were performed in PACs solutions with pH 2.4 (ionic strength = 4.0×10^{-3} mol/kg), pH 5.6 (ionic strength = 1.3×10^{-6} mol/kg), and pH 9.4 (ionic strength = 2.5×10^{-5} mol/kg) adjusted by adding HCl or NaOH. Every reading of the instrument was recorded after three consistent readings were attained.

The XPS spectra were obtained with a PHI Quantera SXM^{TM} XPS scanning microprobe (ΦULVAC-PHI. Inc., Japan) photoelectron spectrometer using Al K_α radiation (energy 1486.6 eV). The X-ray power source was operated at 300 W. The measurements were performed under near vacuum condition, with a pressure lower than 3×10^{-7} Pa. The high-resolution scans were performed over 524–544 eV (O 1s spectra). For calibration purposes, the C 1s electron bond energy corresponding to graphitic carbon was referenced to 284.8 eV.

Acid-base titration method was applied to estimate the number of acid and base groups on the surface of activated carbon samples. Acid/base depletion from 0.1 mol/L HCl and NaOH solutions was performed on each sample to determine the acid/base characteristics of carbons (Barton, 1997).

1.3 Kinetic adsorption measurement

The experiments of BrO_3^- removal by PACs were performed using a bath shaker at 120 r/min. A suitable dose of carbon was introduced into a 250-mL amber glass bottles containing 100 μg/L or 500 μg/L BrO_3^- solution. The pH of BrO_3^- solution was 5.6 unless otherwise stated. Then, they were placed on a shaker table for a specified time and filtered through pre-washed 0.45 μm filters, and the filtrates were analyzed by ion chromatography.

1.4 Maximum adsorption capacity measurement

The maximum adsorption capacity of PACs was obtained using Langmuir isotherm model (Eq. (1)):

$$\frac{1}{q_e} = \frac{1}{q_m} + \frac{1}{k_L q_m} \times \frac{1}{c} \quad (1)$$

where, q_e and c are the concentrations of BrO_3^- in the PACs and equilibrium solution, respectively, q_m represents the maximum adsorption capacity, and k_L is the Langmuir adsorption constant that is related to the adsorption energy. To determine the isothermal (20 ± 1)°C adsorption capacity, 1000 mg/L PACs was added into BrO_3^- solutions with various concentrations. After 24 hr for equilibrium adsorption, 1 mL mixture solution was extracted and filtered through pre-washed 0.45 μm filters for analyzing by ion chromatography.

1.5 Analysis

The BrO_3^- measurement was conducted using an ion chromatography (ICS-1500, Dionex, Canada), which was equipped with a dual-piston pump, an UV/Vis detector (UVD-500, Dionex, Canada), an AS50 autosampler, and IonPac AS23 separator columns (UVD-500, 4 mm, Dionex, Canada). The eluent solution was 9 mmol/L Na_2CO_3. The chromogenic agents were 1.2 mmol/L $NaNO_2$ and the mixture solution of 1.5 mol/L KBr and 1.0 mol/L H_2SO_4. The minimum detection limit for BrO_3^- was 1.2 μg/L. Calibrations were performed before each series of samples was analyzed. The yield of bromine was determined using an ion chromatograph consisting of a pretreatment column (IonPacAG14A-SC, 4 mm, Dionex, Canada), a separator (AS14A-SC, 4 mm, Dionex, Canada), a suppressor (ASRS-ULTRA, 4 mm, Dionex, Canada), and a pulse electronic chemical detector (Dionex, Canada). Na_2CO_3/$NaHCO_3$ (3.5 mmol/L:1 mmol/L) was used as eluting solution at the flow rate of 1.2 mL/min and the injection volume was 25 μL.

2 Results and discussion

2.1 Physical characterization of activated carbon

Table 1 shows the porous properties of carbon samples. All the samples exhibited high surface area and possessed both mesopores and micropores. PAC_F carbon had the highest V_{meso} value (0.38 cm^3/g) and pore volume (0.87 cm^3/g). For the three original carbon samples, the ranking of total pore volume was in accordance with V_{meso} volume as $PAC_W < PAC_C < PAC_F$. These differences are ascribed to the nature of the primary raw material and the manufacturing processes. After thermally reduction with N_2, the pore volume and V_{meso} volume of PAC_F and PAC_W carbons slightly increased, while those of the PAC_C slightly decreased.

The surface area and pore size distributions of carbons those were thermally regenerated with N_2 after saturation adsorption were also examined. The results shown in Table 1 indicated that the surface area and pore volume of all carbons were essentially unchanged after the BrO_3^- adsorption onto these carbons. With thermal regeneration after the BrO_3^- saturation adsorption, the surface area and pore volume of PAC_W were 976.0 m^2/g and 0.79 cm^3/g, respectively, which were slightly higher than those of PAC_W deoxidized with N_2 (the surface area of 880.4 m^2/g and pore volume of 0.66 cm^3/g). Specially, PAC_F and PAC_F deoxidized with N_2 exhibited relatively decrease of surface area and pore volume comparing with their corresponding volumes before BrO_3^- adsorption. The surface area and pore volume of PAC_F decreased from 1102.0 to 940.2 m^2/g and from 0.87 to 0.72 cm^3/g respectively, and the surface area and pore volume of PAC_F deoxidized with N_2 decreased from 1270.0 to 1013.2 m^2/g and from 0.99 to 0.79 cm^3/g respectively. It indicated that the thermally regeneration treatment influenced the textural properties of PAC_F carbons.

Table 2 provides the surface characteristics of selected PACs. The zeta potential and the basicity of the carbons increased with thermal reduction in N_2 environment and with the decrease in BrO_3^- solution pH. The results also showed that coal-based PAC_C had the highest zeta potential value and basicity among three types of original carbons.

2.2 Chemical characterization of activated carbons

The analysis of the contents of oxygen and carbon composition as well as deconvolution results of O 1s core-level XPS spectra of PACs samples are presented in Fig. 1 and Table 3. The O1s core-level spectra indicated that the C=O (about 531.5 eV) and C–O (about 533 eV) groups existed in the samples, whose appearance might be due to the existence of carboxylic acids, lactones, or phenolic species (Pigamo et al., 2002). Clearly, the amounts of oxygen in C=O and total oxygen in PAC_F were the lowest among all original carbons. Additionally, total oxygen

Table 1 Porous properties of the powdered activated carbons (PACs) and PACs treated with N_2 after saturation adsorption

PACs	Surface area (m^2/g)		Pore diameter (nm)		V_{meso} (cm^3/g)		V_{micro} (cm^3/g)		Pore volume (cm^3/g)	
	PACs	PACs treated with N_2	PACs	PACs treated with N_2	PACs	PACs treated with N_2	PACs	PACs treated with N_2	PACs	PACs treated with N_2
PAC_W	828.0	976.0	2.46	2.80	0.24	0.37	0.33	0.42	0.57	0.79
PAC_F	1102.0	940.2	2.55	2.51	0.38	0.31	0.49	0.41	0.87	0.72
PAC_C	688.8	716.1	3.07	3.05	0.33	0.34	0.28	0.28	0.61	0.62
PAC_W deoxidized with N_2	841.1	880.4	2.81	2.66	0.31	0.29	0.36	0.37	0.67	0.66
PAC_F deoxidized with N_2	1270.0	1013.2	2.48	2.45	0.44	0.39	0.55	0.40	0.99	0.79
PAC_C deoxidized with N_2	773.1	711.0	2.95	3.00	0.22	0.25	0.18	0.21	0.40	0.46

Table 2 Surface characteristics of the activated carbons

PACs	Zeta potential (mV)			Basicity (mmol/g)	Acidity (mmol/g)
	pH 2.4	pH 5.6	pH 9.4		
PAC_W	2.1	–6.6	–9.7	0.86	0.18
PAC_F	1.3	–8.7	–17.8	0.52	0.20
PAC_C	2.3	–2.6	–9.5	1.20	0.17
PAC_W deoxidized with N_2	3.4	0.15	–3.6	0.91	0.17
PAC_F deoxidized with N_2	5.6	4.5	–0.4	1.20	0.19
PAC_C deoxidized with N_2	4.9	3.6	–1.3	0.95	0.18

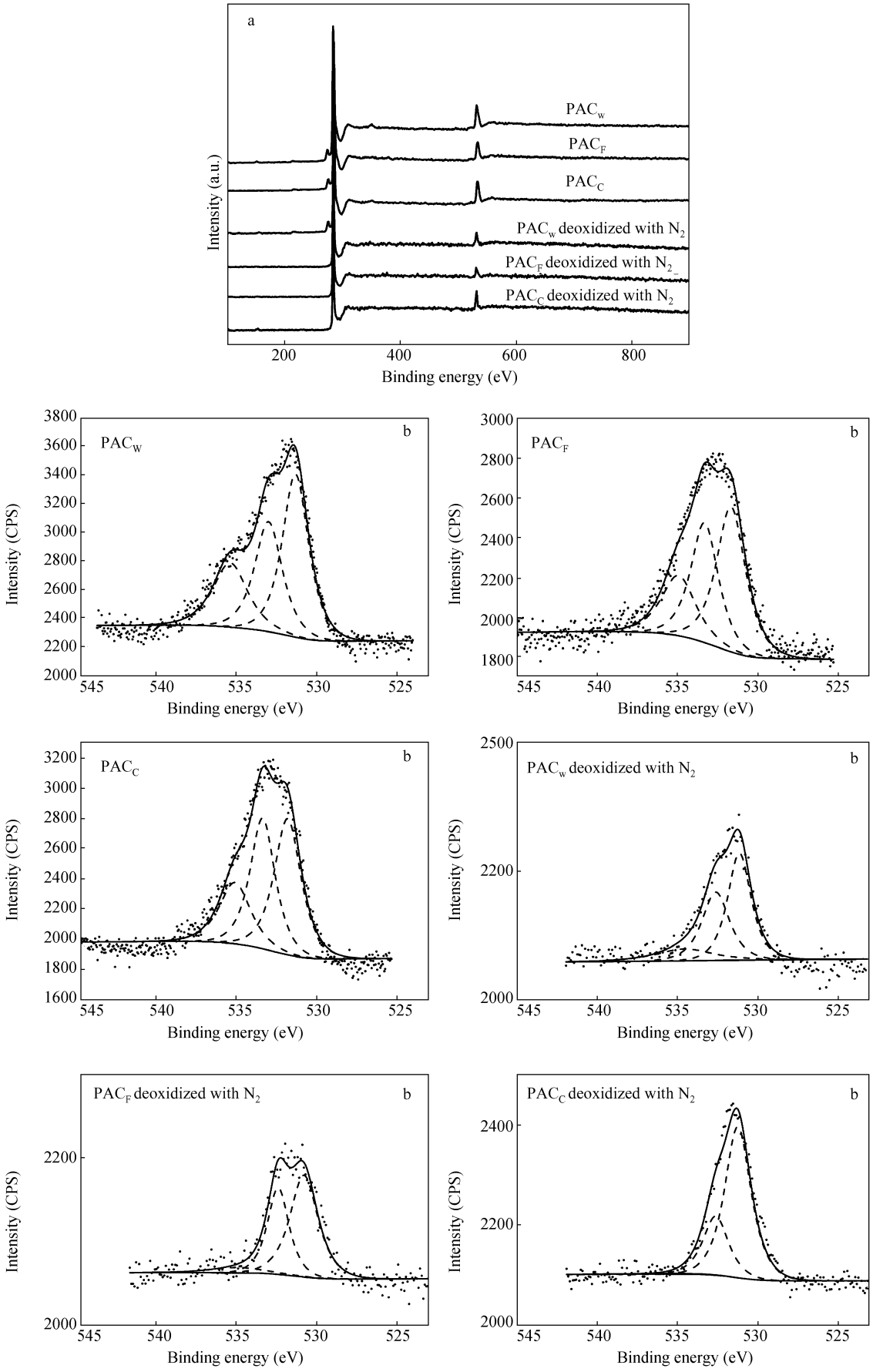

Fig. 1 XPS survey spectra of the PACs samples (a), O1s core-level XPS spectra of the PACs samples (b). The dots represent the actual experimental data; the black lines are the fitting curves and baselines fitted by the Shirley function. The dash lines represent the fitting peaks of C=O and C–O.

Table 3 Distribution of oxygen-bearing structures (at.%) from O 1s core-level XPS spectra (Fig. 1) and the atomic ratios of O and C on PACs surfaces

PACs	Oxygen in groups from O 1s fitting (at.%)			Total O (at.%)	C (at.%)
	C=O	C–O	H_2O adsorbed		
PAC_W	4.03	2.84	2.07	8.94	91.06
PAC_F	2.86	2.23	1.40	6.49	93.51
PAC_C	3.38	3.04	1.77	8.19	91.81
PAC_W deoxidized with N_2	2.28	1.70	0.60	4.58	95.42
PAC_F deoxidized with N_2	1.88	1.22	0.19	3.29	96.71
PAC_C deoxidized with N_2	3.36	1.81	0.01	5.18	94.59

contents, as well as the contents of C=O and C–O groups of PACs deoxidized carbons with N_2 at 600°C declined largely, which means PACs could be deoxidized efficiently through N_2 treatment.

2.3 Adsorption kinetic and adsorption volume studies

Figure 2 presents batch kinetic removal curves of adsorption capacity versus contact time for the six carbons. The adsorption capacity of BrO_3^- by activated carbons varied significantly with the type of carbons, ranging from 0.01 mg/g for PAC_W to almost complete adsorption (0.43 mg/g) for PAC_C within 5 hr, and PAC_F showed a moderate removal rate. As compared with the published results (Siddiqui et al., 1996), PAC_C used in this study showed an excellent efficiency for removal of BrO_3^-. The quickest adsorption of PAC_C might be due to the highest zeta potential, high V_{meso}, and less C=O groups, since surface properties and V_{meso} volume are reported to be important to the adsorption of carbon (Huang et al., 2007; Huang and Cheng, 2008; Siddiqui et al., 1996). The adsorption rate of PAC_W in this study was the lowest, which was contrary with the previous reported results (Huang and Cheng, 2008), this might be owing to the different volume of mesopore, zeta potential, and oxygen content on account of different manufacturing processes. Surely, our reduction method of optimization on the nature of carbons was significant for the study on the adsorption capacity of BrO_3^-. The thermally deoxidized carbons greatly promoted the adsorption rate of carbons through the increases of zeta potential and the obvious decrease of oxygen content.

Figure 3 shows the maximum adsorption capacity of

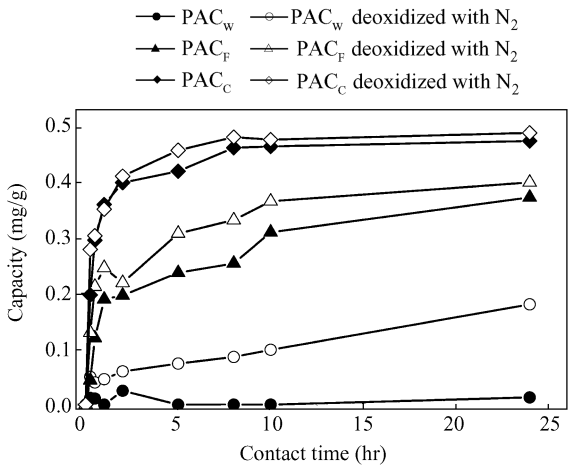

Fig. 2 Effect of the PACs type on BrO_3^- removal. Initial concentration of BrO_3^- and PACs are 100 μg/L and 200 mg/L, respectively.

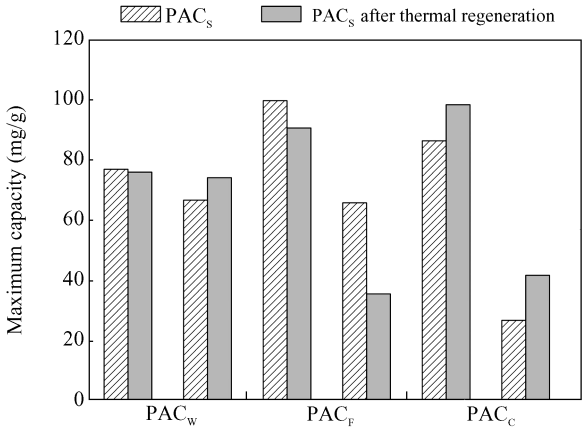

Fig. 3 Maximum adsorption capacity of the PACs and PACs after thermal regeneration for BrO_3^- adsorption.

PACs calculated with Langmuir isotherm model. The maximum adsorption capacity of PAC_F was about 99.6 mg/g, which was the highest saturation adsorption capacity because of its highest pore volume among all tested carbons. It is surprised to note the maximum adsorption capacity of the thermally deoxidized carbons largely decreased. Considering pore volume values of activated carbons, it could be found that the pore volume and V_{meso} volume were somewhat related to their maximum adsorption capacity, However, the reason need to be clarified by further work. Regeneration experiments of carbon samples were also performed. The maximum adsorption capacity of recovered PACs was almost the same to their original state, indicating that the adsorption capacity of PACs could be recovered by thermal regeneration and the recovered carbons could be recycled.

The PAC_C, PAC_F, PAC_C deoxidized with N_2, and PAC_F deoxidized with N_2 were optimally selected in the following experiments considering their high adsorption rates and short-time removal of BrO_3^-. Figure 4 shows pH effects on the removal of BrO_3^-. The removal rate of BrO_3^- increased with the decrease of pH value of BrO_3^- solutions. The negative zeta potential of PACs (Table 2) in high pH solutions was corresponding to the presence of negatively charged carboxylate anionic surface functional groups on the PACs (Siddiqui et al., 1996). In solution with lower pH values, the weakly acidic and basic functional groups were protonated, accompanying with the zeta potential of carbons turning into positive value. As a result, the electrostatic interaction between the carbon and bromate was promoted. The point of zero charge varies among carbons, and the literature describes carbons with points of

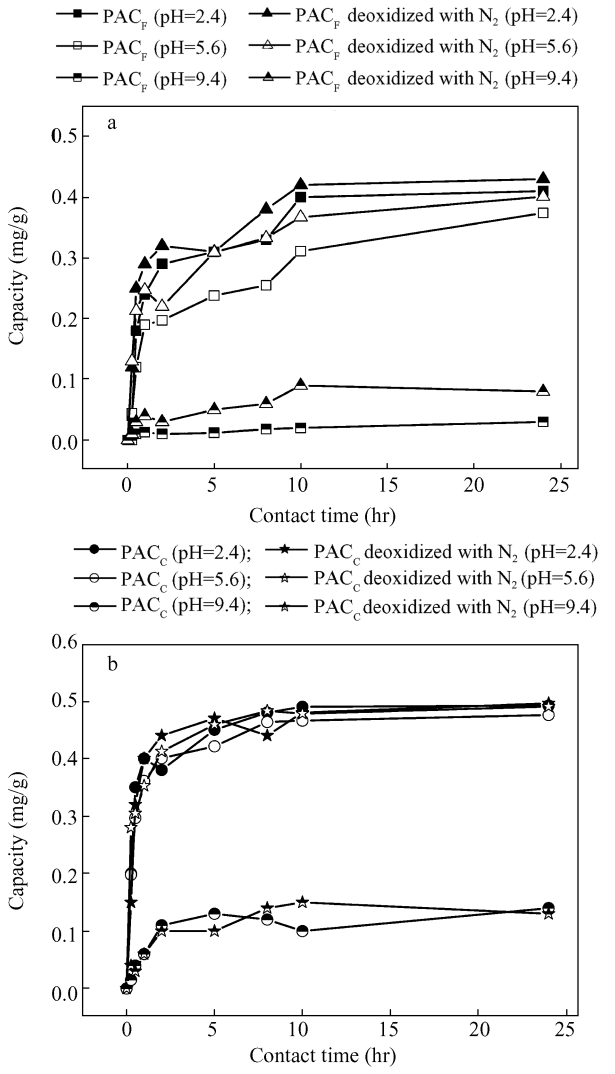

Fig. 4 Effect of pH on BrO_3^- removal by PAC_F (a) and PAC_C (b). Initial concentration of BrO_3^- and PACs are 100 μg/L and 200 mg/L, respectively.

zero charge ranging from approximately 3 to 9 (Karanfil et al., 1998; Siddiqui et al., 1994). Therefore, the electrostatic attraction between bromate and the carbon depend not only on the pH of solution but also on the type of carbon.

The reduction contribution on the BrO_3^- removal by PACs was evaluated. In the batch experiment with PACs, BrO_3^- reduction accompanying with bromide formation were observed (Fig. 5). After 96 hr contact with PACs, 3.9 μmol/L BrO_3^- was almost completely removed and 0.6 μmol/L bromide formed, indicating that approximately 20% of bromate was reduced to bromide and 80% of bromate adsorbed by PACs in the process of BrO_3^- removal. Furthermore, the bromide concentration did not linearly increase as a function of time, which might be due to the adsorption process of bromide onto PACs (Bao et al., 1999). The release and diffusion of bromide in the bromide adsorption process were interactional and competitive, leading that bromide could not immediately release into the solution once formed.

In the process of BrO_3^- removal, the adsorption rate was

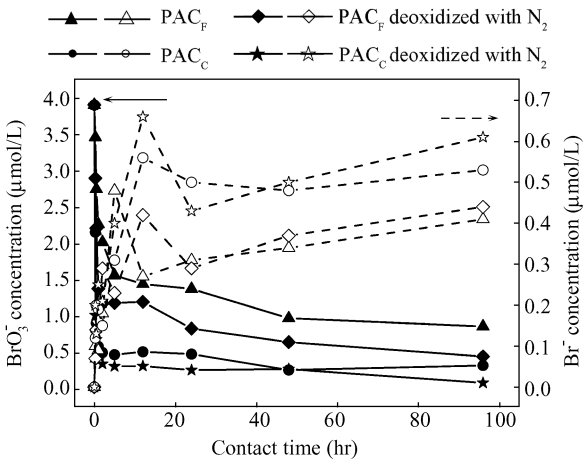

Fig. 5 BrO_3^- adsorption/reduction by the selected PACs and the formation volume of Br^-. Initial concentration of BrO_3^- and PACs are 500 μg/L and 1000 mg/L, respectively.

high at the initial stage and then quickly decreased to a pseudo platform stage (5–96 hr), which was similar to the process of bromide release. On the basis of this, it could be supposed that the adsorption and reaction processes reached pseudo homeostasis in the platform stage. The process of BrO_3^- removal was complex, including the surface and inner diffusion of bromate, adsorption of bromate, formation of bromide, and the release and diffusion of bromide, and so on. The kinetics of adsorption of BrO_3^- on the selected carbons was described using intraparticle diffusion models and pseudo second-order in this work. The validity of the two models could be determined using the linear plots of q_t versus $t^{1/2}$ (Eq. (2)) and t/q_t versus t (Eq. (3)).

$$q_t = k_p t^{1/2} \tag{2}$$

where, k_p is the intraparticle diffusion rate constant, q_t is the amounts of BrO_3^- adsorbed at time t (Wu et al., 2001).

$$\frac{t}{q_t} = \frac{1}{k_2 q_e^2} + \frac{1}{q_e^2} t \tag{3}$$

where, k_2 is the equilibrium rate constant of pseudo second-order adsorption, q_e is the amounts of BrO_3^- adsorbed at equilibrium.

In order to more accurately describe the kinetics, the quick adsorption stage (before 5 hr) and the pseudo platform stage (5–96 hr) of the adsorption curves were simulated separately. Tables 4 and 5 present the correlation coefficient, standard deviation (SD), and standard error (SE) to compare quantitatively the fitness of the models. The values of SD and SE for pseudo second-order kinetics evidently exceed those in the intraparticle diffusion model. Furthermore, the values of q_e (before 5 hr) and q_e' (5–96 hr) calculated with pseudo second-order kinetics were not consistent with the experimental values (Fig. 5). In addition, the intraparticle diffusion model was strongly consistent with the experimental data, suggesting that the adsorption of BrO_3^- on powdered activated carbon was diffusion-controlled.

Table 4 Kinetic parameters of intraparticle diffusion model for the adsorption of BrO_3^- on the selected PACs

PACs	Intraparticle diffusion					
	k_p (mg/(g·hr$^{1/2}$))	SE	SD	k_p' (mg/(g·hr$^{1/2}$))	SE	SD
PAC_F	0.049	0.012	0.013	0.014	0.004	0.026
PAC_C	0.19	0.027	0.029	0.013	0.0019	0.011
PAC_F deoxidized with N_2	0.32	0.079	0.084	0.0037	0.0017	0.010
PAC_C deoxidized with N_2	0.31	0.11	0.11	0.0036	0.0010	0.0063

Table 5 Kinetic parameters of second-order kinetic model for the adsorption of BrO_3^- on the selected PACs

PACs	Second-order kinetic model							
	q_e (mg/g)	k_2 (g/(mg·hr))	SE	SD	q_e' (mg/g)	k_2' (g/(mg·hr))	SE	SD
PAC_F	2.33	0.39	0.73	0.97	0.73	0.40	0.058	4.27
PAC_C	3.93	0.46	0.20	0.27	0.71	0.45	0.038	2.82
PAC_F deoxidized with N_2	10.09	0.49	0.14	0.19	3.88	0.46	0.022	1.63
PAC_C deoxidized with N_2	32.67	0.47	0.021	0.029	1.92	0.49	0.0031	2.29

3 Conclusions

The adsorption capacity and kinetics of BrO_3^- on powdered activated carbon revealed that the characteristics of activated carbon influenced their capacity and rate for the adsorption-reduction process. The efficiency of PACs for BrO_3^- removal depended on the type of PACs, contact time, and pH of BrO_3^- solution. Analysis of various properties of PACs indicated that the carbons with rich mesopores, higher zeta potential value, and lower oxygen content could rapidly and effectively remove the more BrO_3^-. Among the selected carbons, coal-based carbon had a high and an excellent efficiency on adsorption of BrO_3^-. The PACs thermally deoxidized in N_2 atmosphere possessed higher zeta values and contained lower oxygen content than original carbons, leading to the rapid adsorption of BrO_3^-. The reproduction adsorption capacity of PACs could be completely recovered by thermal treatment in N_2 atmosphere and the recovered PACs could be recycled. Under acidic conditions, the PACs possessed high zeta values and adequate basic groups exhibited neutral or positive charges, which had a higher BrO_3^- adsorption capacity. The kinetic data obtained in this study using pseudo second-order and intraparticle diffusion models indicated that the intraparticle diffusion was more applicable model to describe the removal process and the rate determining step was apparently the rate of diffusion of BrO_3^- through the laminar layer surrounding the surface of activated carbon. The combination of zeta potential value, mesopore volume, and oxygen content could be used as the effective indicators for the selection of activated carbon for the removal of BrO_3^-.

Acknowledgments

This work was supported by the National High Technology Research and Development Program (863) of China (No. 2006AA06Z307) and the National Natural Science Found for Creative Research Groups of China (No. 50921064).

References

Bao M L, Griffini O, Santianni D, Barbieri K, Burrini D, Pantani F, 1999. Removal of bromate ions from water using granular activated carbon. *Water Research*, 33: 2959–2970.

Barton S S, Evans M J B, Halliop E, MacDonald J A F, 1997. Acidic and basic sites on the surface of porous carbon. *Carbon*. 35: 1361–1366.

Bouland S, Duguet J P, Montiel A, 2003. Minimizing bromate concentration by controlling the ozone reaction time in a full scale plant. *Ozone: Science & Engineering*, 26: 381–388.

Butler R, Godley A, Lytton L, Cartmell E, 2005. Bromate environmental contamination: Review of impact and possible treatment. *Critical Reviews in Environmental Science and Technology*, 35: 193–217.

Chingombe P, Saha B, Wakeman R J, 2005. Surface modification and characterisation of a coal-based activated carbon. *Carbon*, 43: 3132–3143.

Dollimore D, Heal G R, 1964. An improved method for the calculation of pore size distribution from adsorption data. *Journal of Applied Chemistry*, 14: 109–114.

European Union, 1980. Council directive of 15 July 1980 relating to the quality of water intended for human consumption. *Official Journal of the European Communities*, 23(L229): 11.

Huang W J, Cheng Y L, 2008. Effect of characteristics of active carbon on removal of bromate. *Separation and Purification Technology*, 59: 101–107.

Huang X, Gao N Y, Lu P P, 2007. Bromate reduction by granular activated carbon. *Environmental Science*, 28(10): 2264–2269.

Johnson C J, Singer P C, 2004. Impact of a magnetic ion exchange resin on ozone demand and bromate formation during drinking water treatment. *Water Research*, 38: 3738–3750.

Karanfil T, Kilduff J E, Kitis M, 1998. Removal of DBP precursors and synthetic organic contaminants from water supplies: the role of GAC surface chemistry. In: Proceedings of American Water Works Association Annual Conference, Dallas, Texas. 21–25 June. 423–446.

Kim H, Yamada H, Tsuno H, 2007. The removal of estrogenic activity and control of brominated by-products during ozonation of secondary effluents. *Water Research*, 41:

1441–1446.

Kirisits M J, Snoeyink V L, Kruithof J C, 2000. The reduction of bromate by granular activated carbon. *Water Research*, 17: 4250–4260.

Krasner S W, Glaze W H, Weinberg H, Daniel P, Najm I, 1993. Formation and control of bromate during ozonation of waters containing bromide. *Journal of American Water Works Association*, 85: 73–81.

Lippens B C, de Boer J H, 1965. Pore system *n* catalysts V: the t-method. *Journal of Catalysis*, 4: 319–323.

Marhaba T F, Bengraïne K, 2003. Review of strategies for minimizing bromate formation resulting from drinking water ozonation. *Clean Technology and Environmental Policy*, 5: 101–112.

Pigamo A, Besson M, Blanc B, Gallezot P, Blackburn A, Kozynchenko O et al., 2002. Effect of oxygen functional groups on synthetic carbons on liquid phase oxidation of cyclohexanone. *Carbon*, 40: 1267–1278.

Siddiqui M, Amy G, Ozekin K, Zhai W, Westerho P, 1994. Alternative strategies for removing bromate. *Journal of American Water Works Association*, 86(10): 81–96.

Siddiqui M, Zhai W, Amy G, Mysore C, 1996. Bromate ion removal by active carbon. *Water Research*, 30: 1651–1660.

Studebaker M L, 1957. The chemistry of carbon black and reinforcement. *Rubber Chemistry and Technology*, 30: 1400–1483.

von Gunten U, Hoignè J, 1994. Bromate formation during ozonation of bromide containing waters: Interaction of ozone and hydroxyl radical reactions. *Environmental Science & Technology*, 28: 1234–1242.

Wolf D C, Crosby L M, George M H, Kilburn S R, Moore T M, Miller R T et al., 1998. Time- and dose-dependent development of potassium bromate-induced tumors in male Fischer 344 rats. *Toxicologic Pathology*, 26: 724–729.

WHO (World Health Organization), 1996. Guidelines from Drinking Water Quality (2nd ed.). Chemical and Physical Aspects, Geneva, Swiss. Vol. 2.

Wu F C, Tseng R L, Juang R S, 2001. Adsorption of dyes and phenols from water on the activated carbons prepared from corncob wastes. *Environmental Technology*, 22: 205–213.